Neurobiology of Disease 58 (2013) 3–12

Contents lists available at SciVerse ScienceDirect

Neurobiology of Disease

journal homepage: www.elsevier.com/locate/ynbdi

Neuronal morphology in MeCP2 mouse models is intrinsically variable and depends on age, cell type, and *Mecp2* mutation

I-Ting J. Wang [1], Arith-Ruth S. Reyes [1], Zhaolan Zhou *

Department of Genetics, University of Pennsylvania Perelman School of Medicine, Philadelphia, PA 19104, USA

ARTICLE INFO

Article history:
Received 2 March 2013
Revised 16 April 2013
Accepted 23 April 2013
Available online 6 May 2013

Keywords:
Rett syndrome
MECP2
Neuronal morphology
Dendritic branching
Soma size
Mouse model

ABSTRACT

Rett Syndrome (RTT), a progressive neurological disorder characterized by developmental regression and loss of motor and language skills, is caused by mutations in the X-linked gene encoding methyl-CpG binding protein 2 (*MECP2*). Neurostructural phenotypes including decreased neuronal size, dendritic complexity, and spine density have been reported in postmortem RTT brain tissue and in *Mecp2* animal models. How these changes in neuronal morphology are related to RTT-like phenotype and MeCP2 function, and the extent to which restoration of neuronal morphology can be used as a cellular readout in therapeutic studies, however, remain unclear. Here, we systematically examined neuronal morphology *in vivo* across three *Mecp2* mouse models representing *Mecp2* loss-of-function, partial loss-of-function, and gain-of-function mutations, at developmental time points corresponding to early- and late-symptomatic RTT-like behavioral phenotypes. We found that in *Mecp2* loss-of-function mouse models, dendritic complexity is reduced in a mild, age-dependent, and brain region-specific manner, whereas soma size is reduced consistently throughout development. Neither phenotype, however, is altered in *Mecp2* gain-of-function mice. Our results suggest that, in the cell types we examined, the use of dendritic morphology as a cellular readout of RTT phenotype and therapeutic efficacy should be cautioned, as it is intrinsically variable. In contrast, soma size may be a robust and reliable marker for evaluation of MeCP2 function in *Mecp2* loss-of-function studies.

Introduction

Rett Syndrome (RTT) is a neurological disorder that is caused by mutations in the X-linked gene encoding methyl-CpG binding protein 2 (*MECP2*) (Amir et al., 1999). It primarily affects young girls, with a prevalence of 1 in 10–15,000 live births. One striking feature of RTT is the time course at which clinical symptoms appear. After 6–-18 months of apparently normal development, affected individuals enter a period of developmental stagnation, characterized by microcephaly, growth arrest and hypotonia. This stage is followed by a period of developmental regression, where patients display stereotypic hand wringing and social withdrawal, lose acquired motor and speech skills, and develop respiratory abnormalities (Chahrour and Zoghbi, 2007).

Phenotypic variability is present within the classic RTT profile, where affected girls differ by clinical severity (Chahrour and Zoghbi, 2007). This variability may be attributed to random X-chromosome inactivation and the variety of *MECP2* mutations, including missense, nonsense, deletion, and insertion mutations, that have been identified in RTT patients (Bienvenu and Chelly, 2006). *In vitro* biochemical studies have demonstrated that the majority of these mutations lead to *Mecp2* loss-of-function (Kriaucionis and Bird, 2003). Notably, genetic studies have also identified patients carrying duplication or triplication of *MECP2* (Bienvenu and Chelly, 2006). These patients are classified under *MECP2* duplication syndrome and bear a similar but distinct clinical profile to that of classical RTT (Chahrour and Zoghbi, 2007). Mice carrying two-fold levels of *Mecp2* expression also show behavioral abnormalities (Collins et al., 2004; Luikenhuis et al., 2004), highlighting the importance of MeCP2 dosage and the detrimental effect of *Mecp2* gain-of-function.

Histological analysis of postmortem RTT brain tissue has revealed morphological phenotypes including decreased cellular size with increased cell-packing density (Bauman et al., 1995), decreased dendritic complexity (Armstrong, 2005; Belichenko et al., 1994), and decreased spine density (Belichenko et al., 1994; Chapleau et al., 2009). Interestingly, these changes are selective, as decreased dendritic complexity has been observed in the motor, frontal, and inferior temporal cortices, but not in the visual cortex or hippocampus (Armstrong et al., 1995). Moreover, these changes appear to be cortical layer-specific, even within the same cortical area (Armstrong et al., 1995). No evidence of neuronal degeneration or atrophy has been identified (Armstrong, 2005; Jellinger et al., 1988), indicating that these morphological changes are a consequence of impaired neuronal development or structural maintenance, rather than neurodegeneration. What remains unclear, however, is how mutations in *MECP2* lead to these changes in neuronal

* Corresponding author at: Department of Genetics, University of Pennsylvania, 415 Curie Boulevard, Philadelphia, PA 19104, USA.
E-mail address: zhaolan@mail.med.upenn.edu (Z. Zhou).
Available online on ScienceDirect (www.sciencedirect.com).
[1] These authors contributed equally to this work.

0969-9961/$ – see front matter © 2013 Elsevier Inc. All rights reserved.
http://dx.doi.org/10.1016/j.nbd.2013.04.020

morphology and whether they contribute to RTT disease pathology or are secondary consequences of long-term illness.

To investigate the pathogenic mechanisms underlying RTT, several mouse models harboring different *Mecp2* loss-of-function mutations have been developed and characterized (Brendel et al., 2011; Chen et al., 2001; Goffin et al., 2012; Guy et al., 2001; Jentarra et al., 2010; Pelka et al., 2006; Shahbazian et al., 2002). Although the mouse models recapitulate several RTT clinical features, each *Mecp2* mutation confers a discrete behavioral profile, supporting the link between heterogeneity in *MECP2* mutations and phenotypic variability in RTT. Similarly, underlying cellular structure in *Mecp2* mutant mice differs across *Mecp2* mutation (Belichenko et al., 2008, 2009b). While reduced dendritic complexity, soma size, and spine density are commonly identified in *Mecp2* mutant mice (Belichenko et al., 2009a,b; Fukuda et al., 2005; Kishi and Macklis, 2004; Robinson et al., 2012; Stuss et al., 2012; Tropea et al., 2009), these structural phenotypes also differ by cellular subtype and developmental time point (Chapleau et al., 2012; Fukuda et al., 2005). The extent to which these factors influence cellular structure, however, is not well understood, as the use of different techniques and *Mecp2* mouse models have made direct comparisons across studies difficult (Belichenko et al., 2008, 2009a; Chapleau et al., 2009; Cohen et al., 2011; Fukuda et al., 2005; Jentarra et al., 2010; Kishi and Macklis, 2004; Metcalf et al., 2006; Moretti et al., 2006; Robinson et al., 2012; Stuss et al., 2012; Zhou et al., 2006). For example, reduced spine density has been reported in motor cortex layer II/III and V pyramidal neurons in 3-week-old *Mecp2*-null mice (Belichenko et al., 2009a,b), and in layer V at 8 weeks (Tropea et al., 2009), while no change in spine density has been reported in the somatosensory cortex layer II/III pyramidal neurons in 8-week-old *Mecp2*-null mice (Kishi and Macklis, 2004). Whether these dissimilar findings are consequences of brain region-specific or age-dependent regulation of neuronal morphology is difficult to evaluate, as studies have used different imaging techniques, including Golgi staining, neuron dye labeling, and fluorescent reporters, and different *Mecp2* mutant mice (Chen et al., 2001; Guy et al., 2001). Indeed, Golgi staining has revealed reduced spine density in hippocampus CA1 of 12-week-old *Mecp2*-null mice (Robinson et al., 2012), but DiI labeling shows decreased spine density in the same cells at 1 week, and not at 2 or 7 weeks (Chapleau et al., 2012). A comprehensive and systematic analysis using a single experimental method, therefore, is needed to clarify how age, brain region, and *Mecp2* mutation influence RTT-related neuronal morphology.

Importantly, recent studies have shown that RTT-like symptoms can be ameliorated through the reintroduction of MeCP2 in mice (Giacometti et al., 2007; Guy et al., 2007; Lioy et al., 2011; Robinson et al., 2012). The reversibility of RTT phenotypes has stimulated wide interest in developing cellular assays to measure MeCP2 function. Morphological phenotypes such as spine density, dendritic outgrowth, and soma size have been used as readouts of therapeutic efficacy upon restoration of MeCP2 (Giacometti et al., 2007; Robinson et al., 2012) or IGF-1 treatment in mice and induced pluripotent stem cells (iPSCs) (Marchetto et al., 2010; Tropea et al., 2009). Thus, understanding the relationship between MeCP2 function, neuronal structure, and RTT-like phenotype, as well as identifying robust and reproducible morphological phenotypes as readouts of MeCP2 function, are imperative.

In this study, we systematically analyzed neuronal morphology in three *Mecp2* mouse models, $Mecp2^{-/y}$, $Mecp2^{T158A/y}$, and $Mecp2^{Tg1}$, that represent the spectrum of *MECP2* mutations contributing to the phenotypic heterogeneity of RTT and *MECP2* duplication syndrome. The $Mecp2^{-/y}$ mice lack *Mecp2* and demonstrate the most severe behavioral phenotype, representing *Mecp2* loss-of-function (Guy et al., 2001). The $Mecp2^{T158A/y}$ mice, mimicking a common RTT patient missense mutation at the Threonine 158 residue, demonstrate a moderately severe behavioral phenotype, representing *Mecp2* partial loss-of-function (Goffin et al., 2012). Lastly, the $Mecp2^{Tg1}$ mice express two-fold levels of MeCP2 and are believed to model *MECP2* duplication syndrome, representing *Mecp2* gain-of-function (Collins et al., 2004). Importantly, although neuronal morphology in *Mecp2* loss-of-function models has been individually studied (Belichenko et al., 2008, 2009a; Chapleau et al., 2009; Fukuda et al., 2005; Kishi and Macklis, 2004; Moretti et al., 2006; Robinson et al., 2012; Stuss et al., 2012), a direct comparison of morphological phenotypes in *Mecp2* mouse models across the RTT phenotypic spectrum, including the less severe partial loss-of-function *Mecp2* mutations and *Mecp2* duplication, has yet to be conducted.

Given the progressive nature of RTT-like phenotypic onset, we focused on early and late developmental time points representative of none-to-mild behavioral phenotype ("early" time point) and overt behavioral phenotype ("late" time point) in each mouse model. By using the same experimental method to analyze neuronal morphology *in vivo* across these mouse models and developmental time points, we aimed to address the following questions in this study: 1) The effect of *Mecp2* loss- or gain-of-function on the development of neuronal morphology, 2) The relationship between RTT-like behavioral symptomatic severity and underlying neuronal morphology, and 3) The brain region or cell type-specific effects of *Mecp2* mutation on neuronal morphology.

We found that *Mecp2* loss-of-function reduces dendritic complexity in a brain region-specific manner that correlates with the onset of behavioral phenotype. The degree of changes in dendritic complexity, however, was mild, domain-specific, and dependent on *Mecp2* mutation. In contrast, a significant decrease in soma size upon *Mecp2* loss-of-function persisted throughout development and across both *Mecp2* loss-of-function mutations. *Mecp2* gain-of-function, however, did not affect dendritic outgrowth or soma size, even after onset of gain-of-function behavioral phenotypes, suggesting that changes in cellular structure may not be effective readouts of therapeutics targeted toward *MECP2* duplication syndrome. The subtlety of changes in dendritic outgrowth and the dependence on *Mecp2* mutation, developmental time point, and brain region raise caution in using dendritic complexity as a cellular readout of RTT-like phenotype. Changes in soma size, however, are reproducible and robust, suggesting that soma size may be a more reliable marker in assessing MeCP2 function and therapeutic efficacy in RTT studies.

Materials and methods

Animal husbandry

Experiments were conducted in accordance to the ethical guidelines of the National Institutes of Health and with an approved animal protocol from the Institutional Animal Care and Use Committee of the University of Pennsylvania. To obtain male mice carrying *Mecp2* mutations and *Thy1-GFP/M* transgene, female mice heterozygous for *Mecp2* mutations $Mecp2^{tm1.1Bird}$ ($Mecp2^{-/+}$, (Guy et al., 2001)), $Mecp2^{tm1.1Joez}$ ($Mecp2^{T158A/+}$, (Goffin et al., 2012)), or $Mecp2^{Tg1}$ (Collins et al., 2004) were crossed with *Thy1-GFP/M* reporter mice (Feng et al., 2000). $Mecp2^{-/y}$ and $Mecp2^{T158A/y}$ were maintained on a C57BL/6 background (Charles River). $Mecp2^{Tg1}$ were maintained on a mixed FVB/C57BL/6 background. Mice were genotyped using a PCR-based strategy for *Mecp2* and *Thy1-GFP/M*, as detailed by the Jackson Laboratory.

Immunohistochemistry

Mice were anesthetized with 1.25% Avertin (2,2,2-Tribromoethanol) (wt/vol), transcardially perfused with 0.1 M phosphate buffered saline (PBS) for 1 min, then with 4% paraformaldehyde in 0.1 M PBS (wt/vol) for 10 min, and post-fixed in 4% paraformaldehyde for 1 h at 4 °C. Immunohistochemistry was performed on 200-μm coronal free-floating sections sliced using a Leica VT1000S vibratome. Tissues were rinsed 2 × 5 min with 0.1 M PBS and were blocked with a solution containing 5% normal goat serum, 0.25% Triton X-100 and 0.05% sodium azide for 2 h at room temperature. Tissues were incubated with primary antibody

in blocking solution (chicken antibody to GFP, Aves Labs, 1:1000) overnight at 4 °C. Fluorescence detection was performed using secondary antibody to chicken conjugated to Alexa Fluor-488 (1:1000, Invitrogen) for 2 h at room temperature. Sections were counterstained with DAPI (1:1000, USB) to visualize DNA.

Confocal microscopy

GFP-labeled cells and their entire dendritic tree were detected spanning the depth of the 200-μm slices. For examination of dendritic complexity, somatosensory cortex layer V pyramidal neurons extending their apical dendrites to the pial surface and their basal dendrites into deep layer VI and hippocampal CA1 pyramidal neurons extending their basal dendrites into the *stratum oriens* and their apical dendrites through the *stratum radiatum* and *stratum lacunosum-moleculare* were imaged. Primary somatosensory cortex barrel field between Bregma coordinates −0.6 to −1.34 was analyzed, using the fimbria as an anatomical landmark. Rostral hippocampus between Bregma coordinates −1.34 to −1.94 was analyzed. For examination of soma size, cells located within 50 μm from the surface of the slice with intact somas were imaged and analyzed. Images of apical and basal dendrites were acquired separately with a Leica confocal microscope and Leica AF6000 imaging software using oil immersion 20 × and 40 × objective lenses. Each image was saved as a z-stacked series of optical sections. Four slices per mouse were imaged: 5–10 neurons for layer V somatosensory cortex per mouse and 7–10 neurons for hippocampal CA1 region per mouse were analyzed. All imaging was performed blind to genotype.

Quantitative analysis of neuronal morphology

Z-projection images of individual neurons were compressed into a max projection and dendrites were traced manually using ImageJ software (National Institutes of Health) and NeuronJ, an ImageJ plugin for neurite tracing and quantification (Meijering et al., 2004). Dendritic complexity was measured by performing Sholl analysis (Sholl, 1953), counting the number of dendritic crossings through a series of concentric circles centered at the soma and spaced at 20 μm intervals. Soma size was examined in Leica AF6000 by taking an area measurement of somas outlined manually. All quantification was perfomed blind to genotype.

Statistics

Data are reported as mean ± SEM, and statistical analysis was performed using GraphPad Prism 5.0. Sholl analysis was analyzed by two-way ANOVA with Bonferroni correction, with the independent (genotype and Sholl radius) and dependent variables (number of dendritic crossings). Soma size was analyzed by Student's unpaired *t*-test with Bonferonni correction where necessary.

Results

Neuron imaging strategy

To minimize experimental manipulation and variation in our analysis of neuronal morphology in *Mecp2* mutant mice, we took advantage of a genetic labeling approach that has been successfully utilized in other

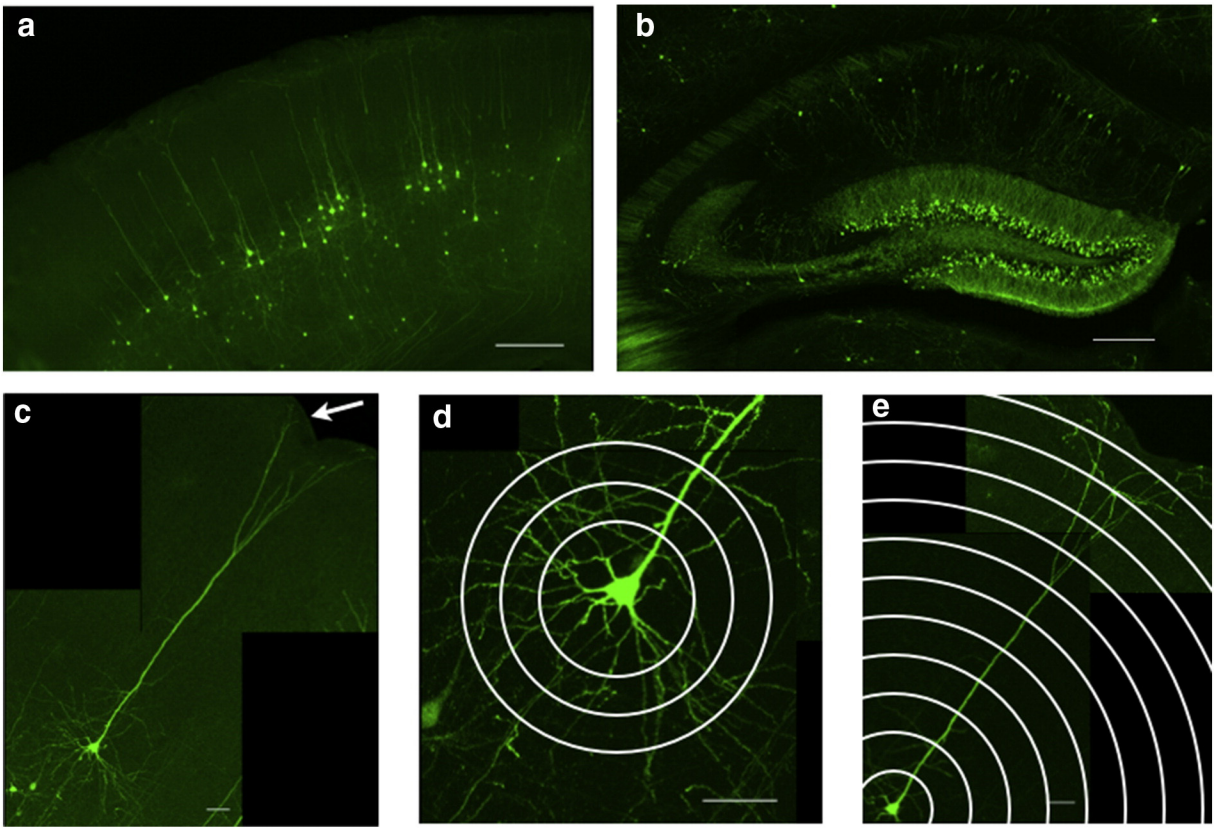

Fig. 1. *Thy1-GFP/M* reporter imaging strategy. (a) Somatosensory cortex layer V pyramidal neurons are labeled with GFP throughout the cell body and dendritic tree in *Thy1-GFP/M* reporter mice. Scale bar = 250 μm. (b) Hippocampus CA1 pyramidal neurons are labeled with GFP throughout the cell body and dendritic tree in *Thy1-GFP/M* reporter mice. Scale bar = 250 μm. (c) Somatosensory cortex layer V pyramidal neurons extend their apical dendrites to the pial surface (arrow) and their basal dendrites deep into layer VI. Scale bar = 50 μm. (d) Basal dendrites of somatosensory cortex layer V pyramidal neurons, quantified by Sholl analysis, measuring number of intersections between concentric circles drawn around the cell soma (Sholl radii) and dendritic branches. Scale bar = 50 μm. (e) Apical dendrites of somatosensory cortex layer V pyramidal neurons, quantified by Sholl analysis. Scale bar = 50 μm.

RTT morphological studies, a *Thy1-GFP/M* reporter line (Belichenko et al., 2009a; Cohen et al., 2011). In this line, a sparse population of neurons intrinsically expresses GFP throughout the cell body and dendritic tree in various brain regions (Figs. 1a, b), allowing for direct visualization of individual neurons (Feng et al., 2000). To visualize neurons in *Mecp2* mutant mice, we crossed male *Thy1-GFP/M* reporter mice to female *Mecp2* heterozygotes ($Mecp2^{-/+}$, $Mecp2^{T158A/+}$, or $Mecp2^{Tg1}$). Given the confounding effects of mosaic *Mecp2* expression in females from random X-chromosome inactivation, all experiments were performed using male littermates with the following genotypes: $Mecp2^{-/y}$; *Thy1-GFP/M* and $Mecp2^{+/y}$;*Thy1-GFP/M*; $Mecp2^{T158A/y}$;*Thy1-GFP/M* and $Mecp2^{+/y}$;*Thy1-GFP/M*; or $Mecp2^{Tg1}$;*Thy1-GFP/M* and $Mecp2^{+/y}$;*Thy1-GFP/M*. For simplicity, we will refer to $Mecp2^{+/y}$;*Thy1-GFP/M* as WT and *Mecp2* mutant mice expressing the *Thy1-GFP/M* transgene as $Mecp2^{-/y}$, $Mecp2^{T158A/y}$, or $Mecp2^{Tg1}$.

Previous studies have shown that disruption of MeCP2 results in deficits in neuronal organization, dendritic complexity and synaptic connectivity in the somatosensory cortex of both postmortem RTT tissue and mice (Cohen et al., 2011; Dani and Nelson, 2009; Kaufmann et al., 2000). We therefore analyzed neuronal morphology in layer V pyramidal neurons of the somatosensory cortex. These neurons are distinct in their cellular architecture, characterized by apical and basal dendritic trees and a pyramid-shaped soma (Spruston, 2008), and thus can be consistently identified. We measured dendritic complexity and soma size in layer V pyramidal neurons extending their apical dendrites to the pial surface and their basal dendrites into deep layer VI (Fig. 1c). Given the anatomic and functional distinctions between basal and apical dendritic arbors (Spruston, 2008), we imaged and quantified basal and apical dendritic complexity separately, using Sholl analysis (Figs. 1d–e), which measures dendritic crossings through a series of concentric circles with increasing radii centered around the cell soma (Sholl, 1953).

Dendritic complexity in Mecp2 loss-of-function mice

The majority of mutations in *MECP2* leading to RTT are loss-of-function mutations (Chahrour and Zoghbi, 2007). Therefore, we first assessed neuronal morphology in *Mecp2*-null mice ($Mecp2^{-/y}$) that lack both *Mecp2* transcript and MeCP2 protein, and represent one of the most phenotypically severe *Mecp2* mutant mice (Guy et al., 2001). Like RTT patients, $Mecp2^{-/y}$ mice show no initial RTT-like phenotype, but begin to develop aberrant gait and reduced mobility around 3 postnatal weeks. By 8 postnatal weeks, $Mecp2^{-/y}$ mice display overt RTT-like phenotypes including hindlimb clasping, tremor, and irregular breathing. We therefore chose to investigate neuronal morphology upon *Mecp2* loss-of-function at P30 and P60, time points representative of early-symptomatic and late-symptomatic RTT-like phenotype, respectively. At the early-symptomatic P30 time point, Sholl analysis of somatosensory cortex layer V pyramidal neurons revealed a statistically significant decrease in dendritic complexity in $Mecp2^{-/y}$ mice relative to WT littermates (WT: $n = 24$ neurons, $Mecp2^{-/y}$: $n = 19$ neurons; $p < 0.0001$) (Fig. 2a). *Post hoc* tests revealed that this decrease was most pronounced in $Mecp2^{-/y}$ mice in both basal and proximal apical dendrites 140–160 μm from soma and in the distal apical tuft 700 μm from soma. As RTT-like behavioral phenotypes in P30 $Mecp2^{-/y}$ mice are mild but present, these data suggest that decreased dendritic complexity accompanies RTT-like behavioral phenotype.

At the late-symptomatic P60 time point, $Mecp2^{-/y}$ mice also showed reduced dendritic complexity (WT: $n = 36$ neurons; $Mecp2^{-/y}$: $n = 31$ neurons; $p < 0.0001$) (Fig. 2b). Although mild, these decreases were more widespread than that of P30 and most pronounced in the basal arbor 100–140 μm from soma and in the distal apical arbor 680–700 μm from soma, where the significant reduction in the apical tuft is likely a reflection of reduced cortical thickness and brain size in these mice (Kishi and Macklis, 2004). Given the overt RTT-like behavioral phenotypes in P60 $Mecp2^{-/y}$ mice, the mild reduction in dendritic complexity is surprising but consistent with reports of normal cortical lamination and organization in 7–10 week-old $Mecp2^{-/y}$ mice (Belichenko et al., 2008; Guy et al., 2001; Metcalf et al., 2006) and unaffected dendritic length and complexity from *in vitro* studies using the same mice (Chao et al., 2007). Therefore, as excitatory input onto proximal dendrites comes primarily from local or adjacent collaterals, while input onto distal dendrites comes from more distant cortical or thalamic projections (Spruston, 2008), our data indicate that the mild but widespread reduction in dendritic complexity across domains results in altered total input onto $Mecp2^{-/y}$ layer V excitatory neurons, both in early-symptomatic and late-symptomatic $Mecp2^{-/y}$ mice.

Dendritic complexity in MeCP2 T158A partial loss-of-function mice

One of the most common *MECP2* missense mutations occurs at Threonine 158, converting it to methionine (T158M) or alanine (T158A). We recently developed and characterized an *Mecp2* T158A knockin mouse and found that $Mecp2^{T158A/y}$ mice show a similar but

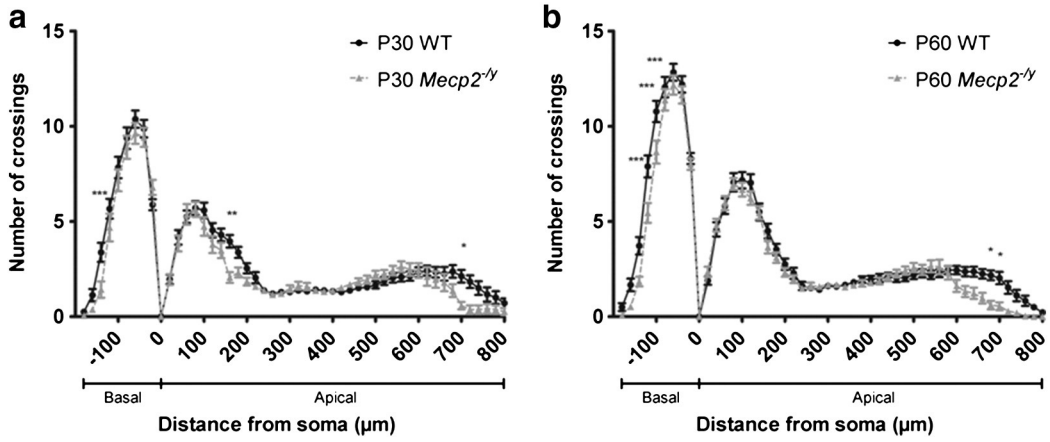

Fig. 2. Dendritic complexity in somatosensory cortex of $Mecp2^{-/y}$ mice. (a) Sholl analysis of somatosensory cortex layer V pyramidal neurons in P30 WT ($n = 24$ neurons from 4 mice) and $Mecp2^{-/y}$ mice ($n = 19$ neurons from 4 mice) shows reduced dendritic complexity in $Mecp2^{-/y}$ mice relative to WT. Basal dendritic arbor is denoted by negative distance from soma, 0 μm marks soma position within cortex, and apical dendritic arbor is denoted by positive distance from soma. Two-way ANOVA with Bonferroni correction, $p < 0.0001$ (interaction); $^{*}p < 0.05$, $^{**}p < 0.01$, $^{***}p < 0.001$. Bars represent mean ± sem. (b) Sholl analysis of somatosensory cortex layer V pyramidal neurons in P60 WT ($n = 36$ neurons from 4 mice) and $Mecp2^{-/y}$ mice ($n = 31$ neurons from 4 mice) show more widespread reduction in dendritic complexity in $Mecp2^{-/y}$ mice relative to WT than seen in P30 animals. Two-way ANOVA with Bonferroni correction, $p < 0.0001$ (interaction); $^{*}p < 0.05$, $^{***}p < 0.001$.

delayed progression of RTT-like behavioral phenotypes relative to that of *Mecp2*$^{-/y}$ mice, where phenotypes begin to develop at 4–5 weeks and are overt by 13 weeks (Goffin et al., 2012). At P60, *Mecp2*$^{T158A/y}$ mice express milder locomotor, anxiety, and motor coordination phenotypes compared to age-matched *Mecp2*$^{-/y}$ mice, indicating that *Mecp2* T158A is a partial loss-of-function mutation. In addition, the *MeCP2* T158A protein is expressed but is less stable and shows reduced binding to methylated DNA (Goffin et al., 2012). To investigate neuronal morphology upon *Mecp2* partial loss-of-function, we measured dendritic complexity at P30, prior to onset of RTT-like phenotypes, and P90, when RTT-like phenotypes are overt. Sholl analysis of layer V pyramidal neurons in the somatosensory cortex of P30 animals revealed a similar pattern of dendritic complexity in *Mecp2*$^{T158A/y}$ and WT littermates (WT: n = 40 neurons; *Mecp2*$^{T158A/y}$: n = 34 neurons; $p > 0.05$; Fig. 3a). Although both *Mecp2*$^{T158A/y}$ and *Mecp2*$^{-/y}$ mice represent *Mecp2* loss-of-function mutations, their RTT-behavioral profiles at P30 are distinct, where RTT-like phenotypes are mild in *Mecp2*$^{-/y}$ mice but absent in *Mecp2*$^{T158A/y}$ mice. These data, therefore, support the hypothesis that decreased dendritic complexity accompanies RTT-like phenotype.

At the late-symptomatic P90 time point, *Mecp2*$^{T158A/y}$ mice showed decreased dendritic complexity relative to WT littermates (WT: n = 36 neurons; *Mecp2*$^{T158A/y}$: n = 39; $p < 0.0001$; Fig. 3B). Strikingly, the decrease was specific to the basal arbor 60–140 μm from soma and was not present in the apical arbor. As pyramidal neuron dendritic domains are believed to receive unique synaptic inputs and contain synapses with distinct properties (Spruston, 2008), the domain-specific decrease in dendritic complexity in *Mecp2*$^{T158A/y}$ mice suggests a cellular mechanism underlying a distinct behavioral profile. Although both P60 *Mecp2*$^{-/y}$ mice and P90 *Mecp2*$^{T158A/y}$ mice show similar RTT-like phenotypic severity, the selective decrease in basal dendritic complexity in *Mecp2*$^{T158A/y}$ mice in contrast to the widespread morphological phenotype seen in *Mecp2*$^{-/y}$ mice supports an *Mecp2* mutation-specific effect on neuronal architecture that may underlie RTT-like phenotypic heterogeneity.

Brain region-specific dendritic complexity in Mecp2 partial loss-of-function

Given the brain region-specific changes in neuronal architecture in RTT postmortem tissue (Armstrong et al., 1995) and compartment-specific changes in *Mecp2* mouse models (Stuss et al., 2012), we next addressed whether the age-dependent and domain-specific decrease in dendritic complexity identified in the somatosensory cortex of *Mecp2*$^{T158A/y}$ mice would be replicated in a different brain region from the same mice. Therefore, we examined neuronal morphology in hippocampal CA1 pyramidal neurons in *Mecp2*$^{T158A/y}$ mice at the pre- and post-symptomatic ages P30 and P90. Similar to what we observed in the cortex, *Mecp2* partial loss-of-function did not affect dendritic complexity in hippocampal CA1 pyramidal neurons at the early-symptomatic P30 time point (WT: n = 27 neurons; *Mecp2*$^{T158A/y}$: n = 33 neurons; $p > 0.05$; Fig. 4a). At the late-symptomatic P90 time point, however, we observed a small but significant change in dendritic complexity in *Mecp2*$^{T158A/y}$ mice (WT: n = 32 neurons; *Mecp2*$^{T158A/y}$: n = 40 neurons; $p < 0.05$; Fig. 4b). *Post hoc* tests revealed that this difference was specific to the basal dendritic arbor, and does not reflect a decrease in dendritic complexity, but rather, is a result of a shift towards the soma, as peak branching in *Mecp2*$^{T158A/y}$ mice is similar to that of controls (Fig. 4c). This shift toward the soma may reflect reduced hippocampal volume, which has been reported in *Mecp2* loss-of-function mice (Belichenko et al., 2008). The age-dependent and domain-specific decrease in dendritic complexity in *Mecp2*$^{T158A/y}$ mice, therefore, is specific to layer V somatosensory cortex and absent in CA1 hippocampus, consistent with RTT postmortem studies (Armstrong et al., 1995). Together, these data support age-dependent and brain region-specific regulation of dendritic outgrowth upon *Mecp2* loss-of-function.

Soma size is regulated throughout development by MeCP2

As both reduced dendritic outgrowth and soma size are believed to contribute to RTT patient microcephaly and reduced soma size has been reported in RTT postmortem tissue (Bauman et al., 1995), we also measured soma size in our *Mecp2* mutant mice at both early- and late-symptomatic time points. In striking contrast to the age-dependence and brain region-specificity of changes in dendritic complexity, we found that changes in soma size persisted throughout development and were consistent between *Mecp2* loss-of-function mutations. Soma size in somatosensory cortex layer V pyramidal neurons was reduced in both P30 early-symptomatic *Mecp2*$^{-/y}$ mice (WT: 282.9 ± 4.0 μm^2, n = 124 neurons; *Mecp2*$^{-/y}$: 237.6 ±4.7 μm^2, n = 103 neurons; $p < 0.01$) and in P60 late-symptomatic *Mecp2*$^{-/y}$ mice (WT: 287.9 ± 4.4 μm^2, n = 126 neurons; *Mecp2*$^{-/y}$: 237.2 ± 4.4 μm^2, n = 104 neurons; $p < 0.01$; Fig. 5a), relative to WT littermates, indicating that *Mecp2* loss-of-function leads to reduced soma size during both early and late development of RTT-like phenotypes. Similarly, soma size was reduced in both P30 pre-symptomatic *Mecp2*$^{T158A/y}$ mice (WT: 290.6 ± 3.9 μm^2, n = 115 neurons; *Mecp2*$^{T158A/y}$: 251.3 ± 4.6 μm^2,

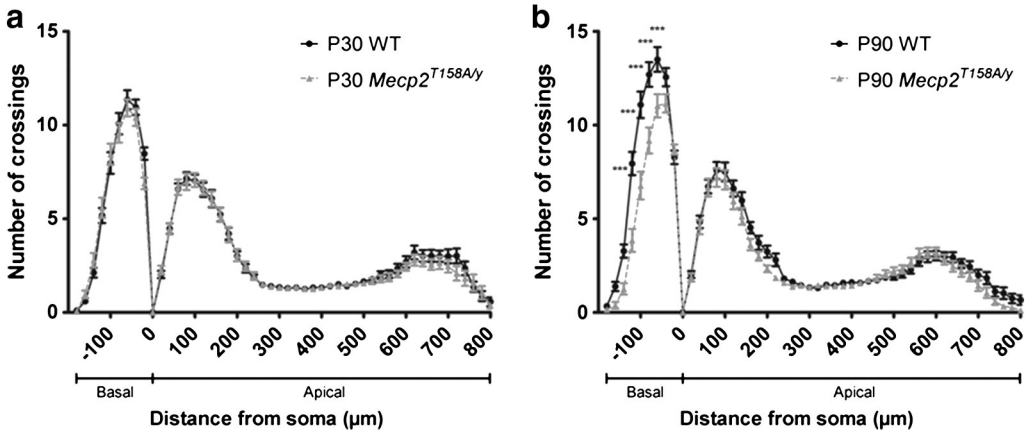

Fig. 3. Dendritic complexity in somatosensory cortex of *Mecp2*$^{T158A/y}$ mice. (a) Sholl analysis of somatosensory cortex layer V pyramidal neurons in P30 WT (n = 40 neurons from 4 mice) and *Mecp2*$^{T158A/y}$ mice (n = 34 neurons from 4 mice) show no change in dendritic complexity in *Mecp2*$^{T158A/y}$ mice relative to WT. Two-way ANOVA, $p > 0.05$. Bars represent mean ± sem. (b) Sholl analysis of somatosensory cortex layer V pyramidal neurons in P90 WT (n = 36 neurons from 4 mice) and *Mecp2*$^{T158A/y}$ mice (n = 39 neurons from 4 mice) show reduced dendritic complexity in *Mecp2*$^{T158A/y}$ mice relative to WT specifically in the basal dendritic arbor. Two-way ANOVA with Bonferroni correction, $p < 0.0001$ (interaction); $^{**}p < 0.01$.

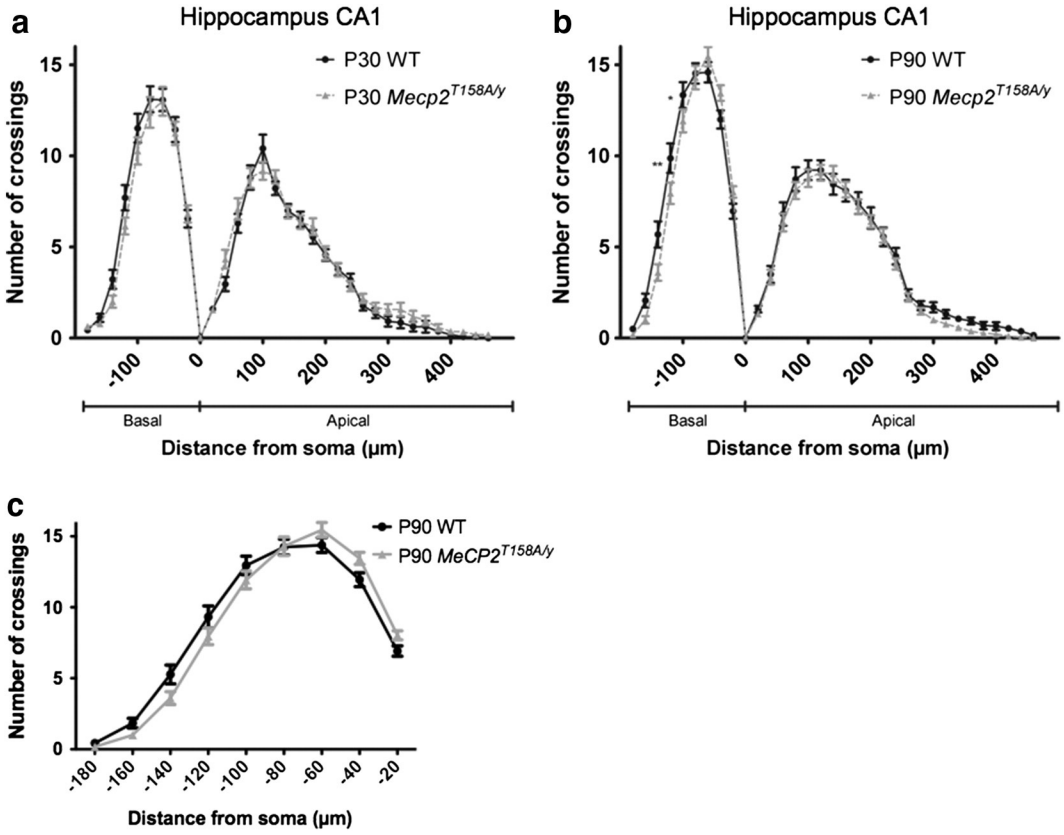

Fig. 4. Dendritic complexity in hippocampus CA1 of *Mecp2*$^{T158A/y}$ mice. (a) Sholl analysis of hippocampal CA1 pyramidal neurons in P30 WT (27 neurons from 5 mice) and *Mecp2*$^{T158A/y}$ mice (n = 33 neurons from 5 mice) show no change in dendritic complexity in *Mecp2*$^{T158A/y}$ mice relative to WT. Two-way ANOVA, $p > 0.05$. Bars represent mean ± sem. (b) Sholl analysis of hippocampal CA1 pyramidal neurons in P90 WT (n = 32 neurons from 5 mice) and *Mecp2*$^{T158A/y}$ mice (n = 40 neurons from 5 mice) show altered dendritic complexity in *Mecp2*$^{T158A/y}$ mice relative to WT specifically in the basal dendritic arbor. Two-way ANOVA with Bonferroni correction, $p < 0.0001$ (interaction); $^{*}p < 0.05$, $^{**}p < 0.01$. (c) Sholl analysis of basal dendritic complexity of hippocampal CA1 pyramidal neurons in P90 WT and *Mecp2*$^{T158A/y}$ mice show no difference in peak number of crossings in *Mecp2*$^{T158A/y}$ mice relative to WT.

n = 121 neurons; $p < 0.01$) and in P90 late-symptomatic *Mecp2*$^{T158A/y}$ mice (WT: 311.1 ± 5.0 μm^2, n = 81 neurons; *Mecp2*$^{T158A/y}$: 262.6 ± 3.3 μm^2, n = 106 neurons; $p < 0.01$) relative to WT littermates (Fig. 5b), indicating that reduced soma size may even precede onset of RTT behavioral phenotypes and is a consequence of *Mecp2* loss-of-function. Moreover, we previously reported that hippocampal CA1 pyramidal neuron soma size is decreased in both pre- and post-symptomatic *Mecp2*$^{T158A/y}$ mice (Goffin et al., 2012). The persistent reduction in soma size in *Mecp2* loss-of-function mouse models throughout development and across different cell types contrasted with the age-dependent and brain region-specific changes in dendritic complexity suggests that MeCP2 regulates dendritic outgrowth and soma size through distinct mechanisms and that soma size may be a more reproducible and reliable cellular marker for MeCP2 function than dendritic complexity.

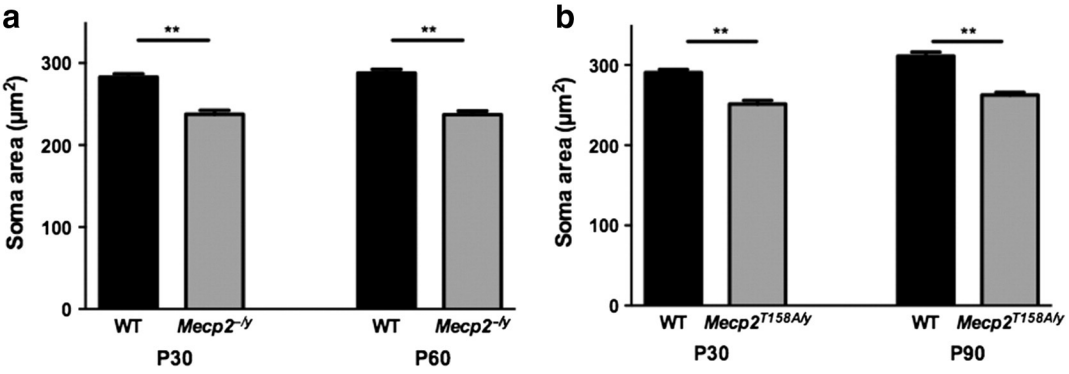

Fig. 5. Soma size is regulated throughout development by MeCP2 function. (a) Somatosensory cortex layer V pyramidal neuron soma size is reduced in *Mecp2*$^{-/y}$ mice relative to WT at both P30 (WT: n = 124 neurons from 4 mice; *Mecp2*$^{-/y}$: n = 103 neurons from 4 mice) and P60 (WT: n = 126 neurons from 4 mice; *Mecp2*$^{-/y}$: n = 104 neurons from 4 mice). $^{**}p < 0.01$, unpaired two-tailed Student *t*-test with Bonferroni correction. Bars represent mean ± SEM. (b) Somatosensory cortex layer V pyramidal neuron soma size is reduced in *Mecp2*$^{T158A/y}$ mice relative to WT at both P30 (WT: n = 115 neurons from 4 mice; *Mecp2*$^{T158A/y}$: n = 121 neurons from 4 mice) and P90 (WT: n = 81 neurons from 4 mice; *Mecp2*$^{T158A/y}$: n = 106 neurons from 4 mice). $^{**}p < 0.01$, unpaired two-tailed Student *t*-test with Bonferroni correction.

Dendritic complexity in Mecp2 gain-of-function mice

As the importance of *MeCP2* dosage has been highlighted though the link between gain-of-function *MECP2* mutations and neurodevelopmental disorder (Chahrour and Zoghbi, 2007), we next examined a transgenic mouse line expressing two-fold levels of MeCP2 ($Mecp2^{Tg1}$) to determine how *Mecp2* gain-of-function affects neuronal morphology (Collins et al., 2004). Importantly, neuronal morphology has yet to be described in *Mecp2* gain-of-function mice. While these mice, similar to that of *Mecp2* loss-of-function models, develop normally, they show enhanced LTP and learning behavior by 20 postnatal weeks and after 30 postnatal weeks, exhibit seizures, ataxia, and premature death (Collins et al., 2004). We therefore examined dendritic complexity and soma size in $Mecp2^{Tg1}$ mice at P30 and P140, time points representative of pre- and post-development of gain-of-function phenotype, respectively. Strikingly, we found similar patterns of dendritic complexity in $Mecp2^{Tg1}$ mice and WT littermates in layer V somatosensory cortex by Sholl analysis at P30 (WT: $n = 16$ neurons; $Mecp2^{Tg1}$: $n = 19$ neurons; $p > 0.05$) (Fig. 6a) and P140 (WT: $n = 23$ neurons; $Mecp2^{Tg1}$: $n = 23$ neurons; $p > 0.05$) (Fig. 6b). These data are in contrast to the reduced dendritic complexity observed in late-symptomatic *Mecp2* loss-of-function animals (Figs. 2b, 3b), and suggest a separate mechanism of dendritic outgrowth regulation in *Mecp2* gain-of-function that is not coupled to behavioral phenotype.

Similarly, we found no changes in soma size in $Mecp2^{Tg1}$ mice relative to WT littermates, both prior to (P30; WT: $266.3 \pm 4.3\ \mu m^2$, $n = 101$ neurons; $Mecp2^{Tg1}$: $272.8 \pm 3.0\ \mu m^2$, $n = 110$ neurons) and after the development of behavioral phenotypes (P140; WT: $268.9 \pm 4.2\ \mu m^2$, $n = 110$ neurons; $Mecp2^{Tg1}$: $265.0 \pm 4.2\ \mu m^2$, $n = 113$ neurons; $p > 0.05$) (Fig. 6c). This finding is consistent with *in vitro* studies showing no effect of MeCP2 overexpression on soma size (Jugloff et al., 2005). Together, these data suggest that neuronal morphology may be affected by *Mecp2* loss-of-function, but is not sensitive to two-fold MeCP2 dosage. This is not surprising, as *MECP2* duplication syndrome is considered to be a separate neurodevelopmental disorder from typical RTT (Ramocki et al., 2009) and likely has a distinct pathogenic mechanism. Neuronal morphology, therefore, may be an appropriate therapeutic readout specifically for RTT patients with *MECP2* loss-of-function mutations.

Discussion

RTT phenotypes are believed to originate from disruptions in neuronal circuits caused by MeCP2 dysfunction in the brain (Goffin and Zhou, 2012; Katz et al., 2012), and changes in neuronal morphology provide a cellular basis for alterations in circuit function. Given the rise in the use of morphological phenotypes as readouts of therapeutic efficacy (Marchetto et al., 2010; Tropea et al., 2009) or restoration of MeCP2 function (Giacometti et al., 2007; Robinson et al., 2012), understanding how *MECP2* mutations impact the maintenance of proper neuronal structure and the relationship between RTT-like phenotype and underlying cellular morphology has become vital. Robust and reproducible RTT-related morphological phenotypes have been difficult to identify, as the use of different techniques, animal models, cell types, and developmental time points across different labs have made direct comparisons between studies difficult. Therefore, we sought to eliminate the confounds of methodological bias by using the same experimental method to analyze neuronal morphology *in vivo* across the development of *Mecp2* loss-of-function, partial loss-of-function, and gain-of-function mouse models. Given the successful utilization of

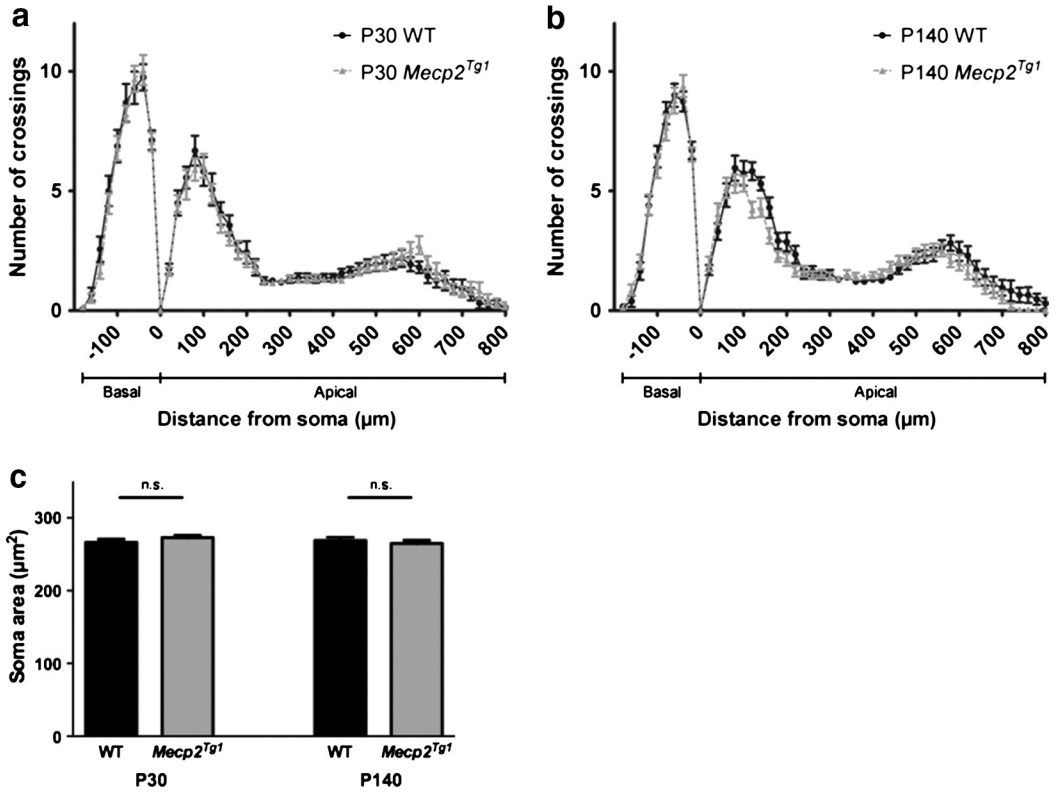

Fig. 6. Dendritic complexity in $Mecp2^{Tg1}$ mice. (a) Sholl analysis of somatosensory cortex layer V pyramidal neurons in P30 WT ($n = 16$ neurons from 2 mice) and $Mecp2^{Tg1}$ mice ($n = 19$ neurons from 2 mice) show no change in dendritic complexity in $Mecp2^{Tg1}$ mice relative to WT. Two-way ANOVA, $p > 0.05$. Bars represent mean ± sem. (b) Sholl analysis of somatosensory cortex layer V pyramidal neurons in P140 WT ($n = 23$ neurons from 2 mice) and $Mecp2^{Tg1}$ mice ($n = 23$ neurons from 2 mice) show no change dendritic complexity in $Mecp2^{Tg1}$ mice relative to WT. Two-way ANOVA, $p > 0.05$. (c) Somatosensory cortex layer V pyramidal neuron soma size is not affected in $Mecp2^{Tg1}$ mice relative to WT at both P30 (WT: $n = 101$ neurons from 2 mice; $Mecp2^{Tg1}$: $n = 110$ neurons from 2 mice) and P140 (P140; $n = 110$ neurons from 2 mice; $Mecp2^{Tg1}$: $n = 113$ neurons from 2 mice). $p > 0.05$, unpaired two-tailed Student *t*-test.

Thy1-GFP/M reporter mice in other cortical and hippocampal morphological studies (Belichenko et al., 2009a; Cohen et al., 2011) and the absence of added experimental manipulations for cellular visualization, we chose to cross our *Mecp2* mutant mice to a *Thy1-GFP/M* reporter line in which neurons are intrinsically labeled with GFP in a mosaic manner throughout several brain regions, including the somatosensory cortex and hippocampus CA1 (Feng et al., 2000). In our study, we aimed to address the following three questions: 1) How does *Mecp2* loss- or gain-of-function affect the development of neuronal morphology? 2) What is the relationship between RTT-like behavioral phenotypic severity and underlying neuronal morphology? 3) Are these changes in neuronal morphology brain region or cell type-specific?

To address the first question, we measured dendritic complexity and soma size in $Mecp2^{-/y}$ and $Mecp2^{T158A/y}$ mice, representing *Mecp2* loss-of-function and *Mecp2* partial loss-of-function, respectively, and $Mecp2^{Tg1}$ mice, representing *Mecp2* gain-of-function. We found decreased dendritic complexity and soma size in *Mecp2* loss-of-function mice ($Mecp2^{-/y}$, $Mecp2^{T158A/y}$) and no change in either phenotype in *Mecp2* gain-of-function mice ($Mecp2^{Tg1}$) relative to WT littermates. These data suggest that MeCP2 expression levels may play a role in the regulation of neuronal outgrowth, but increased MeCP2 expression has no structural effect. Our data also indicate that a greater reduction in MeCP2 may cause more severe morphological defects, as we observed a more widespread reduction in dendritic branching in $Mecp2^{-/y}$ mice, which lack MeCP2 protein (Guy et al., 2001), relative to $Mecp2^{T158A/y}$ mice, which have reduced MeCP2 protein expression (Goffin et al., 2012).

To our knowledge, neuronal morphology has not been studied in *Mecp2* gain-of-function mouse models, and the effect of MeCP2 overexpression *in vitro* on neuronal morphology remains unclear due to reports of increased (Jugloff et al., 2005; Larimore et al., 2009), decreased (Zhou et al., 2006), and unchanged dendritic complexity (Chapleau et al., 2009) in cultured neurons and organotypic slices, and decreased dendritic outgrowth in *Drosophila* and *Xenopus* models (Marshak et al., 2012; Vonhoff et al., 2012). Our findings suggest that both dendritic outgrowth and soma size are reduced upon *Mecp2* loss-of-function, whereas neither phenotype is affected by *Mecp2* gain-of-function with two-fold MeCP2 expression. Notably, $Mecp2^{Tg1}$ mice were maintained on a mixed FVB/C57BL/6 background, and both *Mecp2* loss-of-function models were maintained on a pure C57BL/6 background. Therefore, the different genetic backgrounds may contribute to the differences seen between loss-of-function and gain-of-function models. It is possible that, although two-fold expression of MeCP2 is sufficient to impair synaptic function leading to circuit defects (Chao et al., 2007; Na et al., 2012), it is not sufficient to disrupt cellular morphology *in vivo*. Future study of neuronal morphology in mice expressing three-fold levels of MeCP2 may address this hypothesis, as *MECP2* triplication produces more severe phenotypes both clinically and in mice (Samaco et al., 2012; Van Esch et al., 2007).

To address the second question, the relationship between RTT-like phenotypic severity and underlying neuronal morphology, we measured dendritic complexity and soma size in $Mecp2^{-/y}$ and $Mecp2^{T158A/y}$ mice prior to or at the onset of RTT-like phenotypes (P30) and after development of RTT-like phenotypes. Because RTT-like behavioral progression differs across these mouse models, the ages corresponding to late-symptomatic RTT similarly differed (P60, P90, respectively). Overall, we observed a subtle age-dependent effect of *Mecp2* mutation on dendritic complexity in *Mecp2* loss-of function, where progression of RTT-like behavioral phenotype correlates with underlying cellular changes. At the early-symptomatic P30 time point, only the mildly-symptomatic $Mecp2^{-/y}$ mice showed decreased dendritic complexity, while the pre-symptomatic $Mecp2^{T158A/y}$ mice did not, indicating that early in the development of RTT-like phenotypes, changes in neuronal structure vary across different *Mecp2* mutations and may reflect development of RTT-like behavioral phenotypes. This hypothesis is consistent with findings from a comparative study of brain morphology in two 3-week-old *Mecp2* loss-of-function mouse models, in which $Mecp2^{-/y}$ mice with a more severe RTT-like phenotype exhibited more widespread and marked changes in brain structure than $Mecp2^{-/y}$ mice with a milder RTT-like phenotype (Belichenko et al., 2008).

Similarly, we found greater changes in dendritic complexity in late-symptomatic P60 $Mecp2^{-/y}$ and P90 $Mecp2^{T158A/y}$ mice relative to that of P30. The reduction in dendritic complexity in P60 $Mecp2^{-/y}$ mice was slightly more widespread than that of P30 $Mecp2^{-/y}$ mice, and P90 $Mecp2^{T158A/y}$ showed changes in dendritic complexity that were absent at the pre-symptomatic time point. These data indicate that changes in dendritic outgrowth accompany the development of RTT-like phenotypes upon *Mecp2* loss-of-function and are consistent with RTT postmortem histological data showing a correlation between the degree of morphological abnormality and RTT symptom severity at time of death (Bauman et al., 1995).

The developmental changes in dendritic complexity we identified, however, were relatively mild, compared to reports from other *Mecp2* loss-of-function studies (Kishi and Macklis, 2004; Robinson et al., 2012; Stuss et al., 2012), and limited to specific dendritic domains. This is surprising, as the overt behavioral phenotypes present at both late-symptomatic time points would predict underlying cellular architecture to be severely disrupted. One factor in this subtle dendritic outgrowth phenotype may be experimental bias from the *Thy1-GFP/M* reporter line. While an interaction between MeCP2 and a different reporter transgene *Thy1-YFP/H* has been reported (Stuss et al., 2012), we did not identify GFP-labeling biases in our mice. Our selection of layer V cortical neurons extending their apical tufts to the pial surface, however, could have introduced a bias for analysis of neurons with a less severe morphological phenotype within the *Mecp2* mutant neuronal network. As changes in dendritic morphology have been shown to widely differ between individual neurons within a population (Belichenko et al., 2009b), we cannot exclude the possibility that our experimental method was selective for neurons with intact dendritic structures, resulting in a mild dendritic complexity phenotype.

Data from other *Mecp2* mouse models, however, indicate that changes in dendritic arborization may not reflect the severity of behavioral phenotype. While MeCP2 A140V knockin mice with no obvious RTT-like behavioral phenotypes show decreased dendritic complexity (Jentarra et al., 2010), $Mecp2^{308/y}$ mice with motor, social, and learning deficits that model an MeCP2 early truncation show no changes in dendritic complexity or post-synaptic density in cortical and hippocampal CA1 neurons, both before and after onset of RTT-like phenotypes (Moretti et al., 2006). In addition, a developmental time window may exist in which neuronal morphology is more sensitive to MeCP2 function, as previous work has shown that newborn neurons in the hippocampus are severely affected by *Mecp2* loss-of-function (Smrt et al., 2007). Together, these data suggest that while decreases in dendritic arborization may accompany the development of RTT-like behavioral phenotypes in *Mecp2* loss-of-function, the degree of these changes does not necessarily match the behavioral phenotypic severity and therefore, dendritic arborization may not be a robust and consistent cellular readout of RTT-like phenotype.

In contrast to the intrinsic variability of dendritic outgrowth in *Mecp2* mice, we found that MeCP2 soma size regulation is persistent throughout development and dependent on MeCP2 function. Both *Mecp2* loss-of-function mouse models, $Mecp2^{-/y}$ and $Mecp2^{T158A/y}$, showed decreased soma size at early- and late-symptomatic time points relative to WT, suggesting that soma size decreases upon *Mecp2* loss-of-function but does not change with increasing RTT-like symptomatic severity. These data are consistent with findings from ESC-differentiated neurons, where neurons originating from several lines of *Mecp2* loss-of-function mice show decreased soma size relative to controls throughout the course of neuronal maturation (Yazdani et al., 2012), and can be rescued upon restoration of MeCP2. Together,

these data indicate that soma size is regulated by MeCP2 function throughout development and can be an indicator of MeCP2 function.

To address the third question, whether changes in neuronal morphology are brain region or cell type-specific, we assessed neuronal morphology in a separate brain region by measuring dendritic complexity in hippocampal CA1 pyramidal neurons in pre-and post-symptomatic *Mecp2*$^{T158A/y}$ mice. In contrast to the age-dependent decrease in basal dendritic complexity we observed in somatosensory cortex layer V pyramidal neurons of *Mecp2*$^{T158A/y}$ mice, we found no age-dependent reduction in dendritic complexity of hippocampal CA1 pyramidal neurons. These data are consistent with region-specific morphological phenotypes identified in RTT postmortem brain tissue, where pyramidal neurons of the motor, frontal, and inferior temporal cortices show decreased dendritic complexity, but pyramidal neurons in the visual cortex and hippocampus exhibit no change with respect to age-matched controls (Armstrong et al., 1995; Belichenko et al., 1994). Specificity may even extend to cortical layer, as decreased dendritic arborization has been identified in both basal and apical dendrites of layer V motor cortex cells but only in basal dendrites of layer III motor cortex cells (Armstrong et al., 1995). A comparison of data from different studies also supports a cortical layer-specific regulation of neuronal morphology in mice, where neocortical layer II/III pyramidal neurons show decreased dendritic complexity in both proximal basal and apical dendrites and no change in spine density (Kishi and Macklis, 2004) but layer V pyramidal neurons show decreased dendritic complexity in only proximal basal and distal apical dendrites and decreased spine density (Stuss et al., 2012).

In contrast to the cell type-specific changes in dendritic outgrowth, multiple lines of evidence indicate that soma size is consistent across cell types. We previously reported decreased soma size in hippocampal CA1 pyramidal neurons in both pre- and post-symptomatic *Mecp2*$^{T158A/y}$ mice (Goffin et al., 2012), similar to what we observed in the somatosensory cortex in this study. In addition, decreased soma size has been reported in RTT postmortem brain tissue (Armstrong, 2005) and in the locus ceruleus (Taneja et al., 2009), hippocampus CA2 (Chen et al., 2001), layer II/III somatosensory cortex (Kishi and Macklis, 2004), layer II/III motor cortex (Robinson et al., 2012), and layer V motor cortex (Stuss et al., 2012) of different *Mecp2*-null mouse strains. Moreover, various lines of *Mecp2*-deficient ESC-derived neurons (Yazdani et al., 2012) and RTT patient-derived induced pluripotent stem cells (Marchetto et al., 2010) also show reduced soma sizes, indicating that, in contrast to dendritic arborization, a reduction in soma size upon *Mecp2* loss-of-function is a phenotype that is consistent across cell types and experimental systems. Similarly, our finding that soma size is not affected upon *Mecp2* gain-of-function has also been observed *in vitro* (Jugloff et al., 2005), indicating that the absence of a change in soma size upon *Mecp2* gain-of-function is also conserved across cell types.

This consistent and robust reduction in soma size across studies, *Mecp2* loss-of-function mutations, experimental systems, cell types, and developmental time points, is in sharp contrast to changes in dendritic complexity, which vary across these parameters and can be subtle and context-dependent (Stuss et al., 2012). Therefore, in accordance with a recent study evaluating spine density throughout development in *Mecp2* loss-of-function mice (Chapleau et al., 2012), we caution the use of dendritic complexity as a phenotypic endpoint for therapeutic evaluation, and suggest that soma size may be a more robust and reproducible readout of MeCP2 function. Evidence supporting soma size as a reliable morphologic phenotype comes from existing rescue experiments, where activation of a quiescent *Mecp2* gene in adult mice results in partial restoration of dendritic complexity and length but a full restoration of soma size (Robinson et al., 2012). In addition, postnatal neuron-specific reactivation of MeCP2 is sufficient to rescue hippocampal and cortical soma size in *Mecp2*-deficient mice (Giacometti et al., 2007) and neuronal size is restored by the re-expression of MeCP2 in several strains of MeCP2-deficient ESC-derived neurons (Yazdani et al., 2012). Future studies are needed to understand how soma size and dendritic outgrowth are differentially regulated by MeCP2. It is conceivable that dendritic arborization is more sensitive to the cellular environment, growth factors, and homeostatic regulation, whereas soma size is more directly affected by the function of nuclear proteins such as MeCP2.

Overall, our data indicates that within a population of excitatory neurons in RTT mouse models, *in vivo* changes in dendritic complexity upon *Mecp2* loss-of-function are brain region-specific, correlated with behavioral phenotype, and mild. In contrast, soma size is regulated throughout development and may be a reliable marker for evaluating MeCP2 function and therapeutic efficacy. These phenotypes are specific to *Mecp2* loss-of-function, as *in vivo* morphological changes upon *Mecp2* gain-of-function are absent. The use of neuronal morphology as a cellular readout of RTT phenotype and restoration of neuronal circuitry, therefore, should be cautioned, as morphological phenotypes are intrinsically variable.

Acknowledgments

We thank members of the Zhou laboratory for their critical readings of the manuscript. This work was supported by NIH grants R00 NS058391 (Z.Z.) and T32MH017168-29 (I-T.J.W.) and the International Rett Syndrome Foundation (Z.Z). Z.Z. is a Pew Scholar in Biomedical Science.

References

Amir, R.E., Van den Veyver, I.B., Wan, M., Tran, C.Q., Francke, U., Zoghbi, H.Y., 1999. Rett syndrome is caused by mutations in X-linked MECP2, encoding methyl-CpG-binding protein 2. Nat. Genet. 23, 185–188.
Armstrong, D.D., 2005. Neuropathology of Rett syndrome. J. Child Neurol. 20, 747–753.
Armstrong, D., Dunn, J.K., Antalffy, B., Trivedi, R., 1995. Selective dendritic alterations in the cortex of Rett syndrome. J. Neuropathol. Exp. Neurol. 54, 195–201.
Bauman, M.L., Kemper, T.L., Arin, D.M., 1995. Pervasive neuroanatomic abnormalities of the brain in three cases of Rett's syndrome. Neurology 45, 1581–1586.
Belichenko, P.V., Oldfors, A., Hagberg, B., Dahlström, A., 1994. Rett syndrome: 3-D confocal microscopy of cortical pyramidal dendrites and afferents. Neuroreport 5, 1509–1513.
Belichenko, N.P., Belichenko, P.V., Li, H.H., Mobley, W.C., Francke, U., 2008. Comparative study of brain morphology in Mecp2 mutant mouse models of Rett syndrome. J. Comp. Neurol. 508, 184–195.
Belichenko, N.P., Belichenko, P.V., Mobley, W.C., 2009. Evidence for both neuronal cell autonomous and nonautonomous effects of methyl-CpG-binding protein 2 in the cerebral cortex of female mice with Mecp2 mutation. Neurobiol. Dis. 34, 71–77.
Belichenko, P.V., Wright, E.E., Belichenko, N.P., Masliah, E., Li, H.H., Mobley, W.C., Francke, U., 2009. Widespread changes in dendritic and axonal morphology in Mecp2-mutant mouse models of Rett syndrome: evidence for disruption of neuronal networks. J. Comp. Neurol. 514, 240–258.
Bienvenu, T., Chelly, J., 2006. Molecular genetics of Rett syndrome: when DNA methylation goes unrecognized. Nat. Rev. Genet. 7, 415–426.
Brendel, C., Belakhov, V., Werner, H., Wegener, E., Gärtner, J., Nudelman, I., Baasov, T., Huppke, P., 2011. Readthrough of nonsense mutations in Rett syndrome: evaluation of novel aminoglycosides and generation of a new mouse model. J. Mol. Med. 89, 389–398.
Chahrour, M., Zoghbi, H.Y., 2007. The story of Rett syndrome: from clinic to neurobiology. Neuron 56, 422–437.
Chao, H.-T., Zoghbi, H.Y., Rosenmund, C., 2007. MeCP2 controls excitatory synaptic strength by regulating glutamatergic synapse number. Neuron 56, 58–65.
Chapleau, C.A., Calfa, G.D., Lane, M.C., Albertson, A.J., Larimore, J.L., Kudo, S., Armstrong, D.L., Percy, A.K., Pozzo-Miller, L., 2009. Dendritic spine pathologies in hippocampal pyramidal neurons from Rett syndrome brain and after expression of Rett-associated MECP2 mutations. Neurobiol. Dis. 35, 219–233.
Chapleau, C.A., Boggio, E.M., Calfa, G., Percy, A.K., Giustetto, M., Pozzo-Miller, L., 2012. Hippocampal CA1 pyramidal neurons of Mecp2 mutant mice show a dendritic spine phenotype only in the presymptomatic stage. Neural Plast. 2012, 1–9.
Chen, R.Z., Akbarian, S., Tudor, M., Jaenisch, R., 2001. Deficiency of methyl-CpG binding protein-2 in CNS neurons results in a Rett-like phenotype in mice. Nat. Genet. 27, 327–331.
Cohen, S., Gabel, H.W., Hemberg, M., Hutchinson, A.N., Sadacca, L.A., Ebert, D.H., Harmin, D.A., Greenberg, R.S., Verdine, V.K., Zhou, Z., et al., 2011. Genome-wide activity-dependent MeCP2 phosphorylation regulates nervous system development and function. Neuron 72, 72–85.
Collins, A.L., Levenson, J.M., Vilaythong, A.P., Richman, R., Armstrong, D.L., Noebels, J.L., David Sweatt, J., Zoghbi, H.Y., 2004. Mild overexpression of MeCP2 causes a progressive neurological disorder in mice. Hum. Mol. Genet. 13, 2679–2689.
Dani, V.S., Nelson, S.B., 2009. Intact long-term potentiation but reduced connectivity between neocortical layer 5 pyramidal neurons in a mouse model of Rett syndrome. J. Neurosci. 29, 11263–11270.

Feng, G., Mellor, R.H., Bernstein, M., Keller-Peck, C., Nguyen, Q.T., Wallace, M., Nerbonne, J.M., Lichtman, J.W., Sanes, J.R., 2000. Imaging neuronal subsets in transgenic mice expressing multiple spectral variants of GFP. Neuron 28, 41–51.
Fukuda, T., Itoh, M., Ichikawa, T., Washiyama, K., Goto, Y.-I., 2005. Delayed maturation of neuronal architecture and synaptogenesis in cerebral cortex of Mecp2-deficient mice. J. Neuropathol. Exp. Neurol. 64, 537–544.
Giacometti, E., Luikenhuis, S., Beard, C., Jaenisch, R., 2007. Partial rescue of MeCP2 deficiency by postnatal activation of MeCP2. Proc. Natl. Acad. Sci. U. S. A. 104, 1931–1936.
Goffin, D., Zhou, Z., 2012. The neural circuit basis of Rett syndrome. Front. Biol. 7, 428–435.
Goffin, D., Allen, M., Zhang, L., Amorim, M., Wang, I.-T.J., Reyes, A.-R.S., Mercado-Berton, A., Ong, C., Cohen, S., Hu, L., et al., 2012. Rett syndrome mutation MeCP2 T158A disrupts DNA binding, protein stability and ERP responses. Nat. Neurosci. 15, 274–283.
Guy, J., Hendrich, B., Holmes, M., Martin, J.E., Bird, A., 2001. A mouse Mecp2-null mutation causes neurological symptoms that mimic Rett syndrome. Nat. Genet. 27, 322–326.
Guy, J., Gan, J., Selfridge, J., Cobb, S., Bird, A., 2007. Reversal of neurological defects in a mouse model of Rett syndrome. Science 315, 1143–1147.
Jellinger, K., Armstrong, D., Zoghbi, H.Y., Percy, A.K., 1988. Neuropathology of Rett syndrome. Acta Neuropathol. 76, 142–158.
Jentarra, G.M., Olfers, S.L., Rice, S.G., Srivastava, N., Homanics, G.E., Blue, M., Naidu, S., Narayanan, V., 2010. Abnormalities of cell packing density and dendritic complexity in the MeCP2 A140V mouse model of Rett syndrome/X-linked mental retardation. BMC Neurosci. 11, 19.
Jugloff, D.G.M., Jung, B.P., Purushotham, D., Logan, R., Eubanks, J.H., 2005. Increased dendritic complexity and axonal length in cultured mouse cortical neurons overexpressing methyl-CpG-binding protein MeCP2. Neurobiol. Dis. 19, 18–27.
Katz, D.M., Berger-Sweeney, J.E., Eubanks, J.H., Justice, M.J., Neul, J.L., Pozzo-Miller, L., Blue, M.E., Christian, D., Crawley, J.N., Giustetto, M., et al., 2012. Preclinical research in Rett syndrome: setting the foundation for translational success. Dis. Model Mech. 5, 733–745.
Kaufmann, W.E., MacDonald, S.M., Altamura, C.R., 2000. Dendritic cytoskeletal protein expression in mental retardation: an immunohistochemical study of the neocortex in Rett syndrome. Cereb. Cortex 10, 992–1004.
Kishi, N., Macklis, J.D., 2004. MECP2 is progressively expressed in post-migratory neurons and is involved in neuronal maturation rather than cell fate decisions. Mol. Cell. Neurosci. 27, 306–321.
Kriaucionis, S., Bird, A., 2003. DNA methylation and Rett syndrome. Hum. Mol. Genet. 12 (Spec No 2), R221–R227.
Larimore, J.L., Chapleau, C.A., Kudo, S., Theibert, A., Percy, A.K., Pozzo-Miller, L., 2009. Bdnf overexpression in hippocampal neurons prevents dendritic atrophy caused by Rett-associated MECP2 mutations. Neurobiol. Dis. 34, 199–211.
Lioy, D.T., Garg, S.K., Monaghan, C.E., Raber, J., Foust, K.D., Kaspar, B.K., Hirrlinger, P.G., Kirchhoff, F., Bissonnette, J.M., Ballas, N., et al., 2011. A role for glia in the progression of Rett's syndrome. Nature 475, 497–500.
Luikenhuis, S., Giacometti, E., Beard, C.F., Jaenisch, R., 2004. Expression of MeCP2 in postmitotic neurons rescues Rett syndrome in mice. Proc. Natl. Acad. Sci. U. S. A. 101, 6033–6038.
Marchetto, M.C.N., Carromeu, C., Acab, A., Yu, D., Yeo, G.W., Mu, Y., Chen, G., Gage, F.H., Muotri, A.R., 2010. A model for neural development and treatment of Rett syndrome using human induced pluripotent stem cells. Cell 143, 527–539.
Marshak, S., Meynard, M.M., De Vries, Y.A., Kidane, A.H., Cohen-Cory, S., 2012. Cell-autonomous alterations in dendritic arbor morphology and connectivity induced by overexpression of MeCP2 in xenopus central neurons *in vivo*. PLoS One 7, e33153.
Meijering, E., Jacob, M., Sarria, J.-C.F., Steiner, P., Hirling, H., Unser, M., 2004. Design and validation of a tool for neurite tracing and analysis in fluorescence microscopy images. Cytometry A 58, 167–176.
Metcalf, B.M., Mullaney, B.C., Johnston, M.V., Blue, M.E., 2006. Temporal shift in methyl-CpG binding protein 2 expression in a mouse model of Rett syndrome. Neuroscience 139, 1449–1460.
Moretti, P., Levenson, J.M., Battaglia, F., Atkinson, R., Teague, R., Antalffy, B., Armstrong, D., Arancio, O., Sweatt, J.D., Zoghbi, H.Y., 2006. Learning and memory and synaptic plasticity are impaired in a mouse model of Rett syndrome. J. Neurosci. 26, 319–327.
Na, E.S., Nelson, E.D., Adachi, M., Autry, A.E., Mahgoub, M.A., Kavalali, E.T., Monteggia, L.M., 2012. A mouse model for MeCP2 duplication syndrome: MeCP2 overexpression impairs learning and memory and synaptic transmission. J. Neurosci. 32, 3109–3117.
Pelka, G.J., Watson, C.M., Radziewic, T., Hayward, M., Lahooti, H., Christodoulou, J., Tam, P.P.L., 2006. Mecp2 deficiency is associated with learning and cognitive deficits and altered gene activity in the hippocampal region of mice. Brain 129, 887–898.
Ramocki, M.B., Peters, S.U., Tavyev, Y.J., Zhang, F., Carvalho, C.M.B., Schaaf, C.P., Richman, R., Fang, P., Glaze, D.G., Lupski, J.R., et al., 2009. Autism and other neuropsychiatric symptoms are prevalent in individuals with MeCP2 duplication syndrome. Ann. Neurol. 66, 771–782.
Robinson, L., Guy, J., McKay, L., Brockett, E., Spike, R.C., Selfridge, J., De Sousa, D., Merusi, C., Riedel, G., Bird, A., et al., 2012. Morphological and functional reversal of phenotypes in a mouse model of Rett syndrome. Brain 135, 2699–2710.
Samaco, R.C., Mandel-Brehm, C., McGraw, C.M., Shaw, C.A., McGill, B.E., Zoghbi, H.Y., 2012. Crh and Oprm1 mediate anxiety-related behavior and social approach in a mouse model of MECP2 duplication syndrome. Nat. Genet. 44, 206–211.
Shahbazian, M., Young, J., Yuva-Paylor, L., Spencer, C., Antalffy, B., Noebels, J., Armstrong, D., Paylor, R., Zoghbi, H., 2002. Mice with truncated MeCP2 recapitulate many Rett syndrome features and display hyperacetylation of histone H3. Neuron 35, 243–254.
Sholl, D.A., 1953. Dendritic organization in the neurons of the visual and motor cortices of the cat. J. Anat. 87, 387–406.
Smrt, R.D., Eaves-Egenes, J., Barkho, B.Z., Santistevan, N.J., Zhao, C., Aimone, J.B., Gage, F.H., Zhao, X., 2007. Mecp2 deficiency leads to delayed maturation and altered gene expression in hippocampal neurons. Neurobiol. Dis. 27, 77–89.
Spruston, N., 2008. Pyramidal neurons: dendritic structure and synaptic integration. Nat. Rev. Neurosci. 9, 206–221.
Stuss, D.P., Boyd, J.D., Levin, D.B., Delaney, K.R., 2012. MeCP2 mutation results in compartment-specific reductions in dendritic branching and spine density in layer 5 motor cortical neurons of YFP-H mice. PLoS One 7, e31896.
Taneja, P., Ogier, M., Brooks-Harris, G., Schmid, D.A., Katz, D.M., Nelson, S.B., 2009. Pathophysiology of locus ceruleus neurons in a mouse model of Rett syndrome. J. Neurosci. 29, 12187–12195.
Tropea, D., Giacometti, E., Wilson, N.R., Beard, C., McCurry, C., Fu, D.D., Flannery, R., Jaenisch, R., Sur, M., 2009. Partial reversal of Rett syndrome-like symptoms in MeCP2 mutant mice. Proc. Natl. Acad. Sci. U. S. A. 106, 2029–2034.
Van Esch, H., Jansen, A., Bauters, M., Froyen, G., Fryns, J.-P., 2007. Encephalopathy and bilateral cataract in a boy with an interstitial deletion of Xp22 comprising the CDKL5 and NHS genes. Am. J. Med. Genet. A 143, 364–369.
Vonhoff, F., Williams, A., Ryglewski, S., Duch, C., 2012. Drosophila as a model for MECP2 gain of function in neurons. PLoS One 7, e31835.
Yazdani, M., Deogracias, R., Guy, J., Poot, R.A., Bird, A., Barde, Y.-A., 2012. Disease modeling using embryonic stem cells: MeCP2 regulates nuclear size and RNA synthesis in neurons. Stem Cells 30, 2128–2139.
Zhou, Z., Hong, E.J., Cohen, S., Zhao, W.-N., Ho, H.-Y.H., Schmidt, L., Chen, W.G., Lin, Y., Savner, E., Griffith, E.C., et al., 2006. Brain-specific phosphorylation of MeCP2 regulates activity-dependent Bdnf transcription, dendritic growth, and spine maturation. Neuron 52, 255–269.